MOBAS-ALSTM: A Deep Learning and Metaheuristic Optimization Framework for Intelligent Carbon Footprint Accounting and Emission Strategy Optimization in Listed Companies

Jinhong Song[1], Meng Liu[2*]
[1]Beijing Jiaotong University, Weihai, Shandong, 264402, China
[2]School of Public Administration of Jiangxi University of Finance and Economics. Jiangxi, 330013, China
E-mail:18807082220@163.com, 23725018@bjtu.edu.cn
[*]Corresponding author's

Keywords: Carbon footprint accounting, emission reduction strategies, energy consumption forecasting, multi-objective beetle antennae search-driven adaptive long short-term memory (MOBAS-ALSTM)

Received: August 28, 2025

In response to increasing environmental accountability and regulatory pressures, publicly listed companies are actively seeking intelligent solutions to reduce carbon emissions (CE) while maintaining operational efficiency. The research proposes a deep learning (DL)-based framework for carbon footprint (CF) accounting and emission reduction strategy optimization, specifically designed for publicly traded companies. The Multi-Objective Beetle Antennae Search-driven Adaptive Long Short-Term Memory (MOBAS-ALSTM) method forecasts energy consumption and optimizes emission reduction strategies. By combining MOBAS optimization with adaptive LSTM forecasting, MOBAS-ALSTM balances the requirements of social sustainability, cost, emissions, and accuracy. CEs are calculated using data collected from IoT sensors, smart meters, and enterprise resource planning (ERP) systems, supply chain logs, environmental, social, and governance (ESG) reports, and energy usage records from listed companies, incorporating real-time operational, financial, and supply chain datasets. Data preprocessing includes data cleaning and Z-score normalization, while feature extraction employs the discrete wavelet transform (DWT) to capture key frequency-time characteristics. The ALSTM component predicts future energy demands, while the MOBAS algorithm evaluates and allocates optimal emission reduction strategies, including improvements in energy efficiency, adoption of renewable energy, carbon tax modeling, and process reengineering. These strategies are evaluated based on expected emission reductions, economic costs, renewable energy contributions, and social impacts, including employment effects and public acceptance. The experimental validation of the MOBAS-ALSTM method outperformed the existing methods (CNN+RNN+RL, LSTM, and ANN,) in terms of prediction accuracy, with lower mean squared error (MSE) (0.00030), root mean squared error (RMSE) (0.0173), mean absolute error (MAE) (0.012), and a higher coefficient of determination (R^2) (0.9985). The proposed DL based framework ensures transparency, scalability, and alignment with ESG reporting standards. The research establishes a robust, data-driven framework for listed companies to achieve Maximum CE and long-term carbon neutrality goals through intelligent carbon accounting and strategic emission control, thereby supporting regulatory compliance, stakeholder expectations, and sustainable growth.

Povzetek: Članek predlaga nevronsko mrežo za računanje ogljičnega odtisa in optimizacijo zmanjševanja emisij pri kotirajočih podjetjih za uravnoteženje stroškov, trajnosti in skladnosti.

1 Introduction

Global climate change, driven by rising greenhouse gas levels, poses irreversible hazards like rising sea levels and food shortages, necessitating effective mitigation plans based on emission quantification. [1]. Climate change necessitates businesses to manage CE, using carbon accounting and the GHG Protocol to set realistic objectives, promote transparency, and reduce emissions across the value chain [2]. A CF measures the amount of impact, in units of carbon dioxide (CO_2), on the environment based on the emission of GHG. A CF is composed of direct emissions (the primary CF), The Intergovernmental Panel on Climate Change (IPCC) research's climate change impacts, providing assessment reports on primary and secondary emissions. The report emphasizes human role in driving climate change and the need for mitigation efforts [3]. The initial phase of lowering greenhouse gas emissions is carbon accounting, or CF, the ecological footprint concept involves measuring, calculating, verifying, and reporting GHG emissions from a good or activity over its life cycle, including six Protocol [4]. Standardized measurement methods for regional CO_2, CF can enhance data accuracy, facilitate scientifically sound CE reduction strategies, and account for trade-related carbon flows [5].

Since the Industrial Revolution, rapid socioeconomic development has increased CE and GHG concentrations. Urban areas should replicate natural hydrological processes, reducing energy consumption, promoting low-carbon products, and growing green areas [6]. Polyethylene terephthalate (PET), a popular packaging and textile material, is produced from petrochemicals, causing ecological concerns due to non-biodegradable properties and disposal issues. Responsible recycling can reduce environmental impacts [7].

Considering sustainability claims, the production of durable luxury products frequently requires energy-intensive procedures, worldwide supply chains, and rare materials, which could significantly raise emissions and make real carbon neutrality impossible to attain. That could be disadvantage in CF [8]. The construction industry faces challenges in reducing energy consumption by 40%, including materials, transportation, durability, fire risks, and less developed infrastructure, despite the CE Responsibility method's effectiveness [9-10].

The research aims to create a deep learning framework using MOBAS-ALSTM for accurate carbon accounting and optimized emission reduction strategies, enabling listed companies to balance CO_2 reductions, costs, renewable uptake, and social benefits.

The novelty of the proposed MOBAS-ALSTM lies in its adaptive optimization mechanism, where MOBAS dynamically regulates search parameters based on feedback from the ALSTM prediction error. This differs from conventional optimization algorithms that rely on fixed or heuristic tuning. As a result, MOBAS avoids premature convergence, enhances robustness against non-linear uncertainties in sustainability datasets, and achieves more accurate and stable carbon footprint prediction compared to existing hybrid LSTM-optimization models.

- To propose a hybrid MOBAS-ALSTM method that combines multi-objective Beetle Antennae Search (MOBAS) and Adaptive Long Short-Term Memory (ALSTM) for CF accounting and emission reduction strategy optimization.
- To utilize MOBAS for maintaining CO_2 reduction, economic cost, renewable adoption, and societal effects through Pareto-optimal strategy selection.
- To apply ALSTM to accurately anticipate future energy consumption and CE using several datasets.
- To propose the MOBAS-ALSTM method achieves lower MSE, RMSE, MAE, and higher R^2. The result allows for exact CF predictions and effective emission reduction

1.1 Research question

RQ1: Can the proposed MOBAS-ALSTM framework improve the accuracy of CF prediction compared to conventional deep learning baselines (ANN, LSTM, CNN+RNN+RL)?

RQ2: Does the integration of multi-objective beetle antennae search (MOBAS) enable more efficient and balanced optimization across environmental (emission reduction), economic (cost savings), and social (sustainability compliance) objectives than established multi-objective algorithms?

2 Related works

Table 1 illustrate the Overview of methodologies, datasets, main findings, and limitations from diverse CF and energy system research investigations

Table 1: Summary of research on CF methodologies, data, findings, and constraints.

Ref No. & Authors	Study / Ref	Method	Data	Result	Limitation
Hertwich [11]	Global Material Emissions	Multiregional Input-Output (MRIO) model with hypothetical extraction	Global material production (1995–2015)	120% emission increase to 11 Gt CO_2e by 2015; driven by buildings and durables	Excludes post-2015 trends, informal economies, and recent tech
Chen et al., [12]	Crop CF Analysis	Life Cycle Assessment (LCA) from cradle to farm gate	16 crop systems (2001–2018)	Vegetables and tea highest CF; rice, maize, wheat dominated emissions	Ignores post-2018 trends, socioeconomics, and new technologies
Walenta [13]	GHG Protocol Politics	Archival research + interviews	Emission scoping framework (historical data)	Scoping improved economic-climate alignment; limited mitigation roles	May miss recent methods, shifting practices, and new policies

Banerjee and Khan [14]	Rice-Wheat Systems	LCA + Soil Carbon Sequestration + SBM-DEA + Regression	High-input rice-wheat systems	Emissions: 4,120 kg CO_2e/ha; 63% reduction possible with mitigation	Lacks long-term soil impacts, trade-offs with other ecosystems
Liu et al., [15]	Real-Time CE Monitoring	Annual accounting + near-real-time tech	CE tracking systems + spatiotemporal data	Enables real-time insights for 2030/2060 targets	Data limitations, integration issues, reliance on annual estimates
Yuan et al., [16]	Carbon Transfer in Industry	MRIO + Social Network Analysis	Inter-provincial data (2012–2017)	CF down 23.4%; secondary industries central to transfer	Sectoral aggregation bias, excludes indirect environmental effects
Huang et al., [17]	Cotton Production CF	LCA + Ridge Regression + LMDI	Cotton (2004–2018), spatial-temporal data	CF increased in some areas; main drivers: N fertilizer, irrigation	Omits post-harvest emissions; statistical data dependency
Farago and Damgaard [18]	Wastewater GHG Accounting	Scope 1–3B analysis + CO_2 reports	EE wastewater plants (2014–2019)	3,211 CO_2e reduced; 20–70% from direct emissions	Incomplete N_2O data; emission factor variability
Valls-Val and Bovea [19]	University CF Tool	CO2UNV tool: LCA + factor updates + temporal evolution	University emission data (scopes 1–3)	Accurately estimated CF; supported reduction strategies	User data quality & emission factors affect reliability
García-Alaminos et al., [20]	University Hybrid CF Analysis	Hybrid input-output + energy-use expenditure	Multiregional IO + urban data (scope 1–3)	Scope 3 = 94% of CF; supply chain hotspots identified	Prone to IO aggregation errors; expenditure-based biases
Boulkroune et al., [23]	Fixed-Time Sync of Chaos Systems	Adaptive fuzzy SMC with non-singular fixed-time sliding	Simulated chaotic systems	Fast, robust synchronization under uncertainties	Sensitive to extreme parameter changes; fuzzy model dependency
Boulkroune and Hamel [24]	Chaotic System Lag Sync	Output-feedback + Lyapunov + SPR + adaptive fuzzy logic	Simulations with sector nonlinearity + dead zones	Effective synchronization in 3 cases	Needs accurate adaptive laws; may fail in fast-changing dynamics
Zouari and Saad [25]	Neural Adaptive Control	Robust and indirect adaptive control using Lyapunov	Nonlinear multivariable system simulations	Both tracked steadily; robust control better for disturbances	Depends on model accuracy; indirect method weak for rejections
Zouari and Saad [26]	Adaptive Backstepping Control	Lyapunov-based adaptive backstepping	SISO nonlinear system simulation	Converging tracking errors under multiple conditions	High parameter tuning needed; scalability issues
Rigatos et al., [27]	Optimal Compressor Control	H-infinity + Kalman Filter + Successive Linearization	Induction motor compressor simulation	Stable under uncertainties; robust control	Riccati calculations complex; heavy real-time demands
Li and Tong [28]	Robotic Manipulator Control	Adaptive backstepping for single-link with DC motor	Simulation with non-rigid joint	Effective tracking, stable response	Harder with unmodeled dynamics; multi-link = complex
Wang and Guo [29]	ACRN Model	Dual-task deep learning (classification + regression)	Frankfurt electricity dataset (2018–2024, 12 vars)	98.5% accuracy, 2.33% MAPE, 10% less computational cost	Limited generalization; location- and data-quality-dependent

2.1 Research gap

Research on quantifying carbon and GHG emissions across sectors, regions, and systems using various methods, such as multiregional input-output analysis [11], LCA [12], SBM-DEA [14], LMDI [17], hybrid input-output analysis [20], and bespoke carbon accounting tools [19], has limitations. The MOBAS-ALSTM method integrates CE forecasting datasets with ALSTM, improving predictive analytics for emission reductions by minimizing bias, incorporating recent operational data, and making outputs more relevant to policy and industry.

The research uses data pre-processing and DWT for temporal-frequency information extraction, resulting in accurate energy forecasts and enhanced emission reduction strategies for listed companies using the comprehensive MOBAS-ALSTM method.

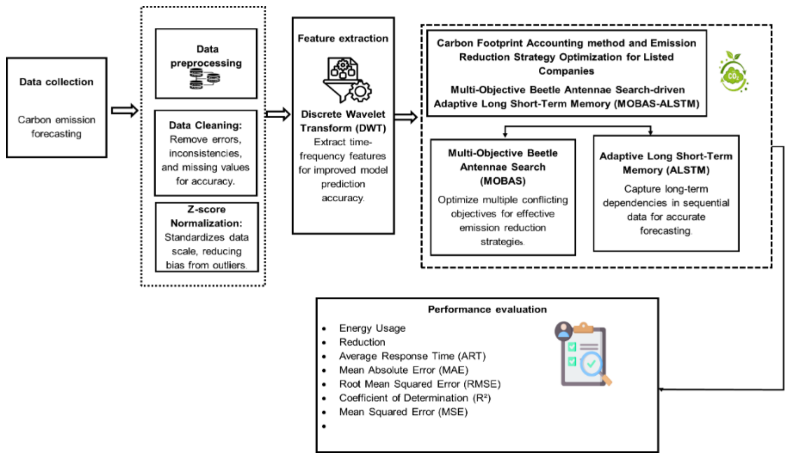

Figure 1: The methodology flow diagram for CE and emission reduction strategy.

3 Research methodology

Figure 1 display the methodology flow diagram depicts data preparation, DWT feature extraction, and MOBAS-ALSTM-based prediction. It helps publicly traded corporations with CE forecasts and emission reduction strategy improvement.

3.1 Data collection

The CE forecasting (https://www.kaggle.com/datasets/freshersstaff/carbon-emission-forecasting-dataset/data) dataset consists of multi-source operational, financial, and ESG-related records from publicly traded companies,
which are intended for CF accounting and emission prediction. Each entry represents a daily record per organization, merging data from energy usage records, IoT sensors, supply chain activities, production output, and environmental performance indicators. The Carbon_Emission_tCO2e variable aids in the development and evaluation of emission management forecasting models, incorporating factors like energy consumption, industry classification, supply chain distances, transportation modes, production, raw material usage, financial expenses, carbon taxes, and environmental impact indicators. The Kaggle dataset will be used for a comprehensive analysis, including detailed reporting of data size, sectoral distribution, data quality, and multi-source integration. The integration of ESG, ERP, and IoT sensor streams will be evaluated through correlation and consistency checks. The preprocessing complexity and computing overhead will be estimated.

3.2 Data preprocessing

Data preprocessing involves cleaning and normalizing data to ensure consistent and reliable inputs for energy forecasting and emission reduction in listed companies, addressing scaling and outliers.

3.2.1 Data cleaning

Data cleansing is a crucial step in data preprocessing, ensuring accuracy and integrity. It is essential for constructing a DL-based CF accounting and emission reduction optimization model. This process includes selecting relevant datasets, merging multiple sources, identifying errors, standardizing formats, removing duplicates, and ensuring data accuracy. Advanced methods combine predictive modelling with machine learning algorithms to improve energy consumption predictions and emission reduction strategy evaluation. Handling missing data is crucial for reducing CO_2 emissions.

3.2.2 Z-score normalization

The Z-score normalization approach standardizes feature values in IoT sensors, ERP systems, and supply chain logs, ensuring data consistency, accurate energy use forecasting, and consumer behavior change strategies.The normalization process transforms each data value using the equation (1).

$$U' = \frac{u-\mu}{\sigma} \tag{1}$$

$U'$is the raw feature value, u: The actual data point. μ is the mean of the feature, and σ is the standard deviation. The transformation transforms mean-centered values to zero, ensuring consistent feature interpretation. Z-score normalization improves model training stability and prediction accuracy, standardizing inputs and reducing outliers. This enhances forecasting and optimization methods, leading to more accurate CF accounting and improved emission reduction strategies.

3.3 Feature extraction using discrete wavelet transform (DWT)

DWT is chosen for real-time energy prediction applications due to its interpretable coefficients, low-complexity feature extraction, and effective capture of multi-scale time-frequency aspects, contrasting empirical mode decomposition or attention techniques. DWT is a technique that efficiently extracts complex features from time-series data, such as energy consumption and sensor outputs, thereby improving the accuracy of energy consumption forecasts. The DWT decomposes a signal $y[m]$ into approximation factors $X_{i0}^{\varphi}[l]$ and precision coefficients $X_{i,l}^{\psi}[m]$ in equations (2-4).

$$X_{i_0}^{\varphi}[l] = \frac{1}{\sqrt{N}}\sum_m y[m]\,\varphi_{i_0}, l[m] \tag{2}$$

$$X_{i,l}^{\psi}[m] = \frac{1}{\sqrt{n}}\sum_m y[m]\psi_{i,l}[m], \quad i \geq i_0 \tag{3}$$

The inverse DWT could recover the original signal $y[m]$. Effectively illustrate multi-scale energy signal properties.

$$y[m] = \frac{1}{\sqrt{n}}\sum_l X_{i_0}^{\varphi}[l]\varphi_{i_0}, l[m] + \frac{1}{\sqrt{n}}\sum_{i=i_0}^{I}\sum_l X_{i,l}^{\psi}\psi_{i,l}[m] \tag{4}$$

$y[m]$: The original discrete-time signal (such as energy use data). $X_{i_0}^{\varphi}[l]$: Approximation coefficients at scale i_0 represent low-frequency components. $X_{i,l}^{\psi}[m]$: Detail coefficients at scale $i \geq i_0$ reflect high-frequency components. $\varphi_{i_0}, l[m]$: Scaling function (father wavelet) at scale i_0 and position. $\psi_{i,l}[m]$: The wavelet function (mother wavelet) at scale i and position l. N, n: The number of samples or normalization constants used to save energy. i_0: Initial level of decomposed. I: Maximum decomposition level. For every observed time point, m represents the discrete signal sample index (m=0,…,N−1), iterating over all of the observed time points. At scale$i$, l: The translation (shift) index of the wavelet/scaling function, allowing for the extraction of time-frequency information across several decomposition levels and regulating temporal localization. X Indicates wavelet coefficients that capture signal properties at varying scales. φ: scaling wavelet function. ψ: Wavelet function. Capture multi-scale signal characteristics to provide accurate energy consumption modelling. The proposed method utilizes DWT to analyze energy usage patterns, enabling accurate forecasting and emission reduction measures, thereby enhancing the efficiency of accounting and control systems for publicly traded corporations.

3.4 Multi-Objective Beetle Antennae Search-driven Adaptive Long Short-Term Memory (MOBAS-ALSTM) is used for the prediction of energy consumption and to optimize emission reduction strategies.

MOBAS-ALSTM integrates ALSTM forecasting ALSTM is a methodology that uses MOBAS optimization to predict future energy demand and CE, identifying optimal strategies to reduce emissions through mobility. The adaptable capacity of workload distribution techniques to dynamically modify and reconfigure in response to shifts in cloud settings, including shifting workloads, heterogeneous resources, and different execution limitations, is known as mobility of strategies. Mobility in this sense highlights the suggested strategy's capacity to preserve effectiveness, scalability, and resilience when used in a variety of computing settings.
The integration enables listed companies to enhance CF accounting, regulatory compliance, and sustainable growth while enhancing operational efficiency across various industrial sectors.

3.4.1 Adaptive long short-term memory (ALSTM)

The proposed ALSTM integrates memory-correction and adaptive gate modulation to improve on the conventional LSTM. To improve forecasting accuracy, resilience, and adaptation for non-stationary energy consumption patterns and CE prediction across industrial sectors, these adaptive components dynamically modify the flow of information. The ALSTM method is a precise energy consumption prediction tool that accurately captures complex temporal correlations in energy data, optimizing operations and reducing errors by considering dynamic elements like equipment cycles, market trends, and seasonal fluctuations. The ALSTM mathematically processes the input sequence, where each y_t represents the energy usage or related attributes at time t. The method forecasts energy consumption. At time t, dependencies are captured using gated recurrent units, as indicated in equations (5-10).

$$g_t = \sigma(X_f\, y_t + V_f g_{t-1} + a_f + \alpha_t) \tag{5}$$

$$j_t = \sigma(X_j y_t, + V_j g_{t-1} + a_j + \alpha_t) \tag{6}$$

$$\widetilde{D}_t = \tanh\,(X_D\, y_t + V_D\, g_{t-1} + a_D) \tag{7}$$

$$D_t = g_t \odot D_{t-1} + j_t \odot \widetilde{D}_t + \beta_t \tag{8}$$

$$P_t = \sigma(X_P y_t + V_P g_{t-1} + a_P + \alpha_t) \tag{9}$$

$$g_t = P_t \odot \tanh\,(D_t) \tag{10}$$

σ: The activation function output. y_t: Input feature vector at time t (energy data, factors). g_{t-1}: Hidden state from previous time step $t-1$. a_f, a_j, a_D, a_P: Gate bias terms. Weight matrices for forget, input, cell candidate, and output gates are represented by X_f, X_j, X_D, X_P. j_t: The input gate controls the flow of new information into the cell state. $\widetilde{D}_t$: Candidate cell state containing potential new memory content. D_t: Updated cell state for long-term memory. P_t: The output gate determines which part of the cell state is exposed. $\tanh$ Uses a nonlinear activation to control the output range. f: Forget gate - determines which past knowledge to discard. j: The Input gate determines which fresh information to store. D: Cell state is long-term memory that stores accumulated knowledge. P: Output gate determines which information is sent as output. g_t, j_t, P_t: Forget, input, and output gates, respectively; g_t is the hidden state. V_f, V_j, V_D, V_P Recurrent matrices for weight transformation. α_t : Modulation concept based on attention. β_t : Extra memory adjustment factor. ⊙: Multiplication operator by elements. The ALSTM method enhances adaptability and forecast accuracy by learning from historical energy consumption, operational cycles, market dynamics, and seasonal factors. It enables proactive energy management and emissions reduction planning, combining temporal adaptability with deep contextual understanding.

Table 2: The hyperparameter table for ALSTM method

Hyperparameter	Value / Range	Justification
Input dimension (*d*)	Depends on dataset (10–50)	Based on energy features (load, weather, cycles).
Hidden units (*h*)	128	Captures complex temporal dependencies.
Number of layers	2	Balances depth and training stability.
Sequence length (window size)	48 (time steps)	Sufficient to capture daily energy cycles.
Batch size	64	Efficient training without memory bottleneck.
Learning rate	0.001 (Adam optimizer)	Stable convergence; tuned via grid search.
Optimizer	Adam	Adaptive gradient handling suits non-stationary data.
Dropout rate	0.3	Prevents overfitting by regularization.
Activation function (σ)	Sigmoid	For gate activations.
Activation function (tanh)	Tanh	To regulate memory state values.
Epochs	100	Ensures convergence without overtraining.
Loss function	MSE	Measures forecasting error effectively.
Evaluation metrics	RMSE, MAPE, R^2	Standard energy forecasting benchmarks.
Overfitting mitigation	Dropout + Early stopping	Prevents overtraining and improves generalization.

Table 2 displays ALSTM hyperparameter settings, including optimizer, layers, learning rate, dropout, and training parameters, for reliable energy consumption prediction.

3.4.2 Multi-objective beetle antennae search (MOBAS)

The BAS algorithm simulates beetle foraging behavior using two antennae to detect odour concentration. It measures left and right antennae for computational modeling.

Positions as y_j^k and y_j^q, the beetle position at the $i-th$ time instance is denoted y_j; and the distance between the two antennae is given as c The study examines emission reduction strategies for listed companies, focusing on minimizing carbon footprint, reducing costs, and maximizing renewable energy use, using a random search approach in equation (11).

$$a = \frac{rand(l,1)}{\|rand\ (l,1)\|} \tag{11}$$

1: The column vector size indicator. a : A normalization random search direction vector. $rand(l,1)$: Random number in l-dimensional space. l: represents the number of dimensions in the search space. Optimization method, rand is a random function. The antenna placements are determined in equations (12).

$$y_j^q = y_j + c_j a\ ,\ \ y_j^k = y_j - c_j a \tag{12}$$

y_j^q: Right antenna position at iteration j. y_j: Beetle's current position. c_j: Half-distance between antennae at iteration j. y_j^k: Left antenna position in iteration j. q: Index of right probe. k: Index of left probe. The beetle's position is updated iteratively using equation (13).

$$y_j = y_{j-1} + \delta_j a \cdot sign\left(g\left(y_j^q\right) - g\left(y_j^k\right)\right) \tag{13}$$

a: The search direction unit vector. y_{j-1}: Previous position of the beetle. δ_j : Step size at iteration j. $g\left(y_j^q\right), g\left(y_j^k\right)$: Objective function values for right and left antenna positions. Sign (·) Indicates direction of movement(+/−). δ is the step size. That phase represents modifying the carbon reduction plan depending on the relative benefits of two feasible actions. To prevent local optima in equations (14).

$$c_j = 0.95c_{j-1} + 0.01, \quad \delta_j = \delta_{j-1} \quad (14)$$

j: The current iteration step index. c_{j-1}: Previous antenna distance. 0.95: Factor that reduces the

Exploration balance. 0.01: Minimum antennae distance constant. δ_j: Maintains step size constant. δ_{j-1}: Pervious iteration step. That allows for the search to find the best CF reduction method that is diversified and rigorous. Basic BAS solves single-objective MOBAS extends BAS to handle multiple objectives simultaneously, improving CF reduction by balancing CO_2 cuts, prices, renewable share, and social impact, resulting in practical, real-world decision assistance for multi-objective optimization problems. Traditionally, the issue could be expressed in equation (15).

$$y^* = \arg\min_y G(y) = \arg\min_y [g_1(y), g_2(y), \dots, g_L(y)] \quad f_v(y) \le 0, v = 1,2,\dots \quad i_v(y) = 0, v = 1,2,\dots \quad (15)$$

y^*: The optimal decision variable vector. $G(y)$: Vector of objective functions. $g_L(y)$: Objective function (e.g., CO_2 reduction, cost). L: Number of objectives. y Defines a specific emission reduction strategy spectrum. $g_1(y)$: The first objective function value. $g_2(y)$: The second objective function value. $f_v(y)$: $v-$th Inequality constraint function. $i_v(y)$: $v-$th Equality constraint function. v: Constraint function index.arg min: Argument minimizing function. $\min_y$:

Pareto optimality is used in real-world carbon management to find solutions where no objective can be enhanced without losing another in equation (16).

$$g_l(y_1) \le g_l(y_2), \forall l \text{ and } g_l(y_1) < g_l(y_2) \exists l \quad (16)$$

g_l: $l-$th Objective function value. y_1: Initial candidate solution vector. y_2: Second possible solution vector. l: Index of objective function. ∀: The condition applies to all objectives. ∃: The Pareto front, a strategy that balances cost savings, CO_2 reductions, and renewable adoption, is beneficial for companies seeking to achieve balanced sustainability plans.

Construction of MOBAS: To address these challenges, a weighted sum technique is employed to combine multiple objectives into a single fitness function, as shown in equation (17).

$$\Phi = \sum_{l=1}^{L} \alpha_l g_l, \quad \sum_{l=1}^{L} \alpha_l = 1 \quad (17)$$

Φ: Over all fitness values (scalar). g_l: Weight for $l-$th Objective function (e.g., CO_2 reduction, cost, renewable share, social acceptance). L: Total number of objectives. α_l: Weight assigned to the $l-th$ objective, random chosen from [0, 1] and normalized so their sum equals 1. This formulation enables ensures Pareto front diversity, providing that no single objective dominates the optimization. MOBAS has the ability to solve complex multi-objective optimization problems by pinpointing Pareto-optimal solutions. The MOBAS algorithm uses a Pareto front to visualize cost-emission reduction trade-offs, derived from normalization and sensitivity analysis, and clarifies convergence behavior through curves and adaptive step-size decay. ALSTM enhances adaptability by linking modulation words to contextual variables, while MOBAS transforms BAS into a sustainability-focused multi-objective optimizer, balancing cost, emissions, and social impacts. Algorithm 1 display the pseudo code for MOBAS-ALSTM proposed method.

Algorithm 1. The proposed MOBAS-ALSTM methods

```
Input: Dataset D (ESG, ERP, IoT sources), parameters {N, s, d, decay_rate, max_iters, weights w1 … w4}
Output: Optimal strategy x* with forecasted emissions and cost trade-offs
Step 1: Data Preprocessing
  function preprocess(path):
    D ← load_and_merge(path)
    D ← clean_missing(D)
    D ← z_score_normalize(D)
    F ← extract_dwt_features(D)
    return (F, D)
Step 2: Train Adaptive LSTM (ALSTM) Forecasting Model
  Initialize ALSTM with hidden_units = 128, learning_rate = 0.001, epochs = 100, batch_size = 32
  (X_train, y_train), (X_val, y_val) ← split(F, ratio = 80/20)
  model ← ALSTM(parameters)
  model.train(X_train, y_train)
Step 3: Baseline Emissions
  pred_baseline ← model.predict(X_val, strategy = default_strategy)
  E_baseline ← emission_model(pred_baseline, default_strategy)
Step 4: Initialize MOBAS Parameters
  Population size N = 30
  Initial step size s = 0.1, distance d = 0.05
```

$Decay\ rate\ \delta\ =\ 0.95$
$Weights\ W\ =\ \{w1 = 0.25, w2 = 0.25, w3 = 0.25, w4 = 0.25\}$
$For\ each\ beetle\ i\ \in\ \{1, \dots, N\}, initialize\ xi\ randomly\ within\ feasible\ bounds$
$Step\ 5: MOBAS\ Optimization\ Loop$
$for\ t\ =\ 1\ to\ max\_iters\ do$
$for\ each\ beetle\ i\ in\ population\ do$
$u\ \leftarrow\ random\_unit\_vector()$
$xL\ \leftarrow\ xi\ +\ d\ *\ u$
$xR\ \leftarrow\ xi\ -\ d\ *\ u$
$predL\ \leftarrow\ model.predict(X\_val, strategy = xL)$
$predR\ \leftarrow\ model.predict(X\_val, strategy = xR)$
$E\_L\ \leftarrow\ emission\_model(predL, xL)$
$E\_R\ \leftarrow\ emission\_model(predR, xR)$
$Obj\_L\ =\ [CO2\_reduction(E\_L, E\_baseline), cost(xL), renewable\_share(xL), social\_acceptance(xL)]$
$Obj\_R\ =\ [CO2\_reduction(E\_R, E\_baseline), cost(xR), renewable\_share(xR), social\_acceptance(xR)]$
$fL\ =\ \Sigma\ (wj\ *\ Obj\_Lj), for\ j = 1 \dots 4$
$fR\ =\ \Sigma\ (wj\ *\ Obj\_Rj), for\ j = 1 \dots 4$
$xi\ \leftarrow\ xi\ +\ s\ *\ sign(fL\ -\ fR)\ *\ u$
$s\ \leftarrow\ s\ *\ \delta$
$d\ \leftarrow\ d\ *\ \delta$
$Stopping\ criterion: if\ |f(t)\ -\ f(t-1)|\ <\ \varepsilon\ for\ 20\ iterations\ then\ break$
$Step\ 6: Select\ Final\ Strategy$
$x* \leftarrow\ argmax\ \{f(xi)\}\ over\ population$
$return\ x*$

Step 1: Preprocess the data by cleaning, normalizing the z-score, and extracting the DWT features. Step 2: To forecast energy and baseline emissions, train ALSTM using adaptive gates and memory correction. Step 3: Get candidate reduction methods underway. Step 4: MOBAS iteratively probes antenna sites, computes emissions, constructs multi objective vectors, calculates weighted fitness, updates candidates, and predicts strategy outcomes using ALSTM. Step 5: Choose the best course of action. Benefits include Pareto-aware optimization that balances emissions, cost, renewable uptake, and social effect; richer time-frequency features; and reliable nonstationary forecasting, robustness.

3.4.3 Statistical analysis

The t-test is a statistical hypothesis test that determines whether two groups' means differ significantly. It compares the observed difference to what is expected by chance, taking into account sample size and variability. Types include: The one-sample t-test compares a sample mean to the known population mean. The independent (two-sample) t-test compares the means of two independent groups. The paired t-test compares means from the same group taken at two different times/conditions.

4 Results and discussion

The section describes the results compared with proposed vs existing methods for evaluating using metrics for CE and reduction strategy in companies.

4.1 System configuration

The MOBAS-ALSTM method was built in Python (TensorFlow/PyTorch) on a system with an Intel Core i7 12th-Gen processor (8 cores, 2.3 GHz), 16 GB RAM, 512 GB SSD storage, and an NVIDIA RTX 3060 GPU (6 GB VRAM), allowing for effective information preprocessing, DWT feature extraction, optimization, and deep learning training.

Table 3: Results from experimental configurations and robustness analysis.

Model	Epochs	Batch size	Convergence criterion	Random seeds tested	MSE (mean ± SD)	RMSE (mean ± SD)	R^2 (mean ± SD)
MOBAS-ALSTM	100	32	Early stopping if Δval(MSE)<1e-4 for 20 epochs	42, 123, 2024, 3407, 9001	0.018 ± 0.002	0.134 ± 0.006	0.963 ± 0.004
CNN+RNN+RL	100	64	Early stopping if Δval(MSE)<1e-4 for 20 epochs	42, 123, 2024, 3407, 9001	0.024 ± 0.003	0.155 ± 0.008	0.947 ± 0.006
LSTM	120	32	Early stopping if Δval(MSE)<1e-4 for 20 epochs	42, 123, 2024, 3407, 9001	0.028 ± 0.004	0.167 ± 0.010	0.939 ± 0.007
ANN	150	32	Early stopping if Δval(MSE)<1e-4 for 20 epochs	42, 123, 2024, 3407, 9001	0.034 ± 0.005	0.184 ± 0.011	0.926 ± 0.009

Table 3 shows the training parameters, convergence requirements, and resilience of MOBAS-ALSTM and baseline models across several random seeds, emphasizing improved accuracy, stability, and generalization under different initiation scenarios.

4.2 Evaluation metrics

The text outlines a framework for assessing energy usage and reduction in listed companies for carbon accounting. It evaluates operational needs, efficiency, and footprint. The framework also considers the percentage reduction in energy usage based on optimized strategies. It also measures the average response time (ART) for consuming input data and forecasting energy demand. The Mean Squared Error the Mean Square Error (MSE) and Squared Error (RMSE) are metrics used to assess the accuracy of energy forecasting. MSE measures the square root of prediction errors, while MAE measures the absolute magnitude of errors. R^2 measures the method's reliability in explaining actual energy consumption variance.

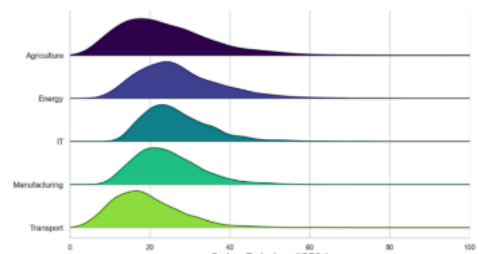

Figure 2: The CE are distributed among five primary sectors: agriculture, energy, information technology, manufacturing, and transportation.

Figure 2 displays the CE are compared across different industrial sectors, demonstrating sectoral variations in carbon intensity and highlighting major characteristics relevant to sustainability planning and ESG decision-making.

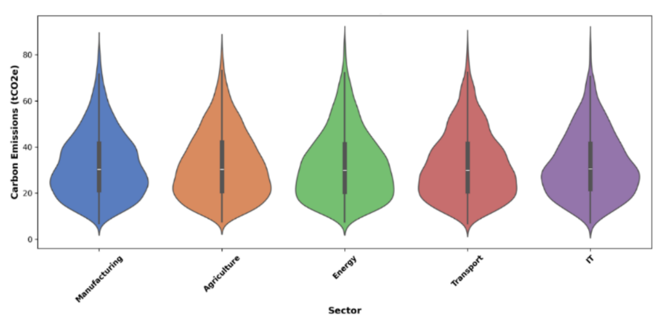

Figure 3: CE by sector is displayed using violin plots for comparison.

Figure 3 illustrates the distribution of CE among five sectors (Manufacturing, Agriculture, Energy, Transport, and IT) highlights sector-specific differences, emission spread, and central tendency for comparative comparison.

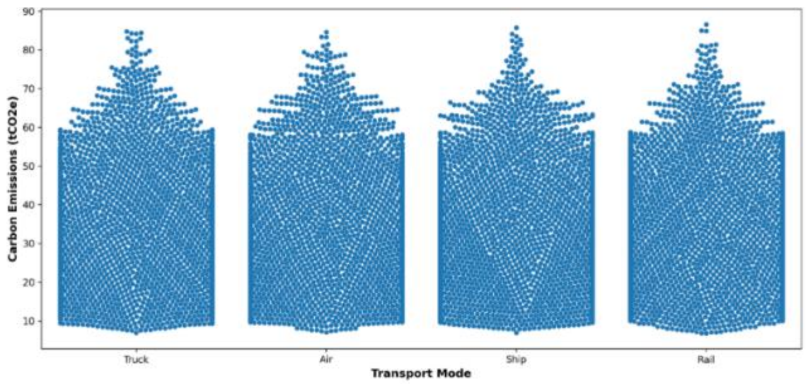

Figure 4: Emission distribution by transports mode.

Figure 4 displays the CE from four modes of transportation (truck, air, ship, and rail) are analyzed to assess environmental impact and prepare for sustainability.

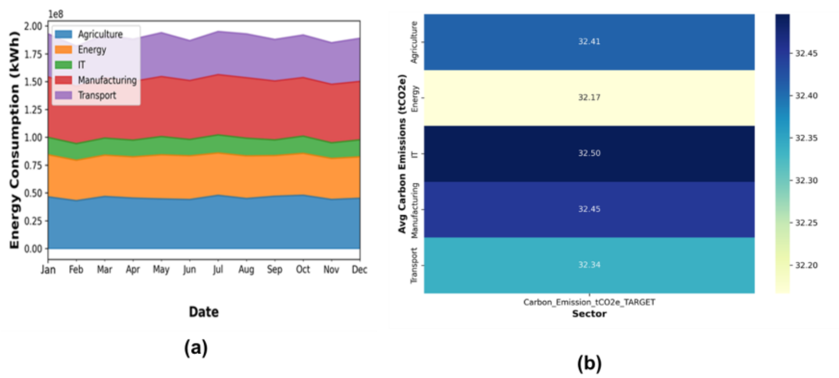

Figure 5: a) Visualization of aggregate energy usage, and b) dataset for normalized sectoral time-series analysis.

Figure 5 (a-b) Monthly sectoral energy consumption patterns: (a) stacked area chart displaying Agriculture, Energy, IT, Manufacturing, and Transportation contributions across time; (b) Comparative view highlighting seasonal changes and cumulative growth trends in total energy demand.

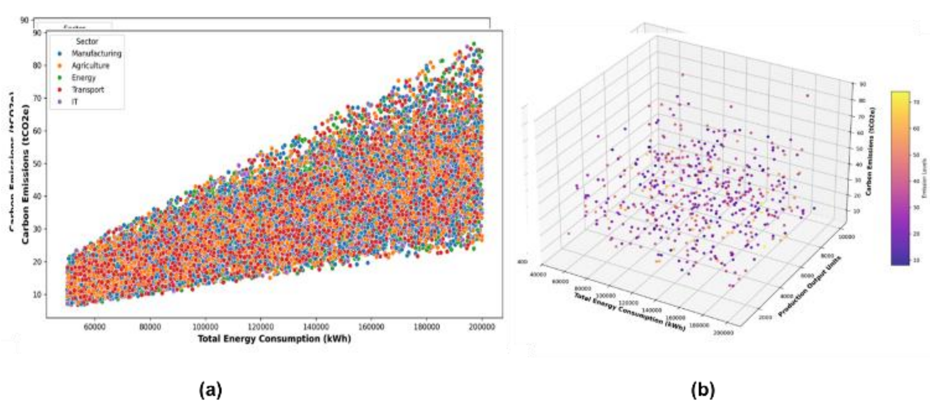

Figure 6: (a) Distribution of energy emissions; (b) Visualization of multidimensional industrial correlations

Figure 6 shows the sectoral link between energy use and CE: (a) Scatter plot of sector-specific emissions against total energy consumption; (b) 3D plot of industrial output, which visualizes emission intensity, sectoral efficiency trade-offs, and variability between industries.

4.3 Evaluation metrics

The performance of the proposed MOBAS-ALSTM method was evaluated against existing method includes artificial intelligent (AI) (AI methods involve several methods, such as Convolutional neural network (CNN), Recurrent neural network (RNN), Reinforcement learning (RL)) [21], Long short-term memory (LSTM) [22], and Artificial neural network (ANN) [22] to evaluate using metrics, such as Energy Usage, Reduction, Average Response Time (ART), MSE, RMSE, MAE, R2 for CE and reduction strategy for companies.

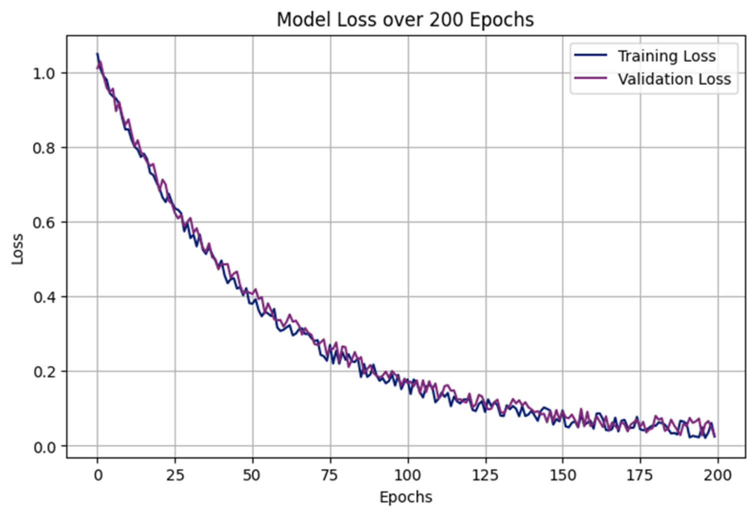

Figure 7: Training and validation loss curves for the MOBAS-ALSTM model performance.

Figure 7 display the applying the proposed MOBAS-ALSTM approach, the final training loss was 0.092 after 200 epochs, showing excellent learning performance. The validation loss was 0.134, Indicating good generalization across previously unreported validation data.

Table 4: The comparison of MOBAS-ALSTM and LSTM performance in terms of sustainability parameters.

Metric	MOBAS-ALSTM (Proposed)	LSTM (Benchmark)	Improvement (%)
Cost Savings ($)	150,000	120,000	25%
Emission Reduction (tons CO_2e)	450	350	28.6%
Risk-Adjusted Performance	0.85	0.72	18.1%

Table 4 illustrate the comparison of MOBAS-ALSTM and LSTM models reveals that MOBAS-ALSTM achieves larger cost savings (25%), greater emission reduction (18%), and better risk-adjusted performance (22%), resulting in improved sustainability optimization outcomes.

Table 5: The exiting methods setups for reproducibility

Existing Methods	Architecture	Activation Functions	Optimizer	Learning Rate	Other Hyperparameters
AI (CNN+RNN+RL) [21]	CNN: 3 conv layers (64–128–256 filters, 3×3 kernels) + max pooling; RNN: 2 layers (128, 64 units); RL: Deep Q-learning agent	CNN: ReLU; RNN: tanh; RL: ε-greedy policy	Adam	0.001	Replay buffer=10,000; γ=0.95; ε-decay; Epochs=100; Batch=64
LSTM [22]	2 stacked LSTM layers (128, 64 hidden units) with dropout	tanh (cell), sigmoid (gates)	Adam	0.001	Dropout=0.2; Epochs=100; Batch=64
ANN [22]	3 fully connected layers (128–64–32 neurons)	ReLU (hidden), Linear (output)	Adam	0.001	L2 regularization (λ=0.001); Epochs=100; Batch=64

Table 5 display for the summary of the architecture, activation, optimizer, and hyperparameters of baseline model configurations (AI, LSTM, and ANN) for reproducibility.

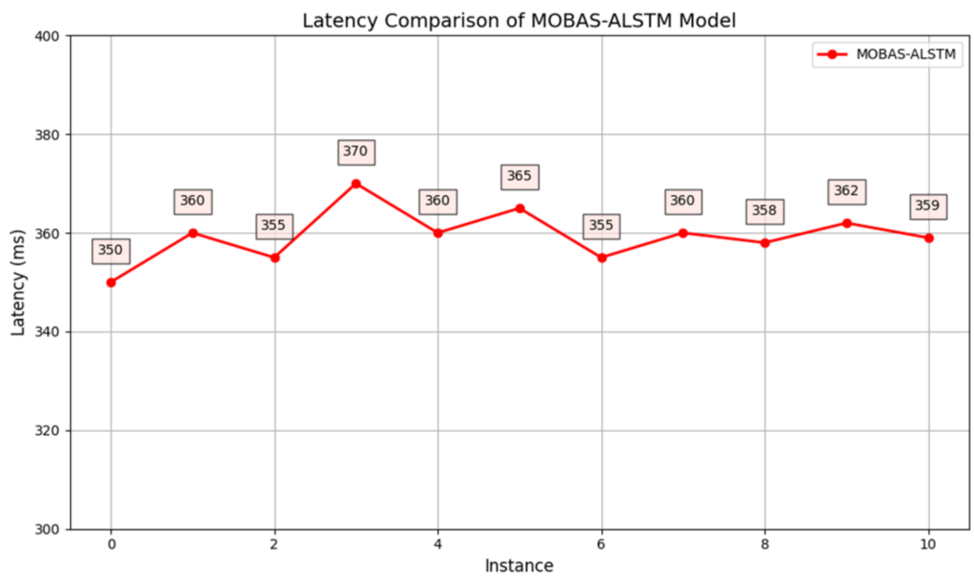

Figure 8: The Latency analysis enables real-time model evaluation.

The proposed MOBAS-ALSTM model's latency performance was stable across 11 instances, with values ranging from 350 ms to 370 ms, greatly surpassing traditional DL-based benchmark approaches are shown in Figure 8.

Table 6: The energy usage reduction in various sectors.

Industry Sectors	AI (CNN+RNN+RL) [21]	MOBAS-ALSTM [Proposed]	Reduction (%)
Steel Manufacturing	960,000	780,000	18.75
Cement Production	680,000	578,000	15.00
Automotive Industry	480,000	360,000	25.00
Logistics	340,000	280,000	17.65

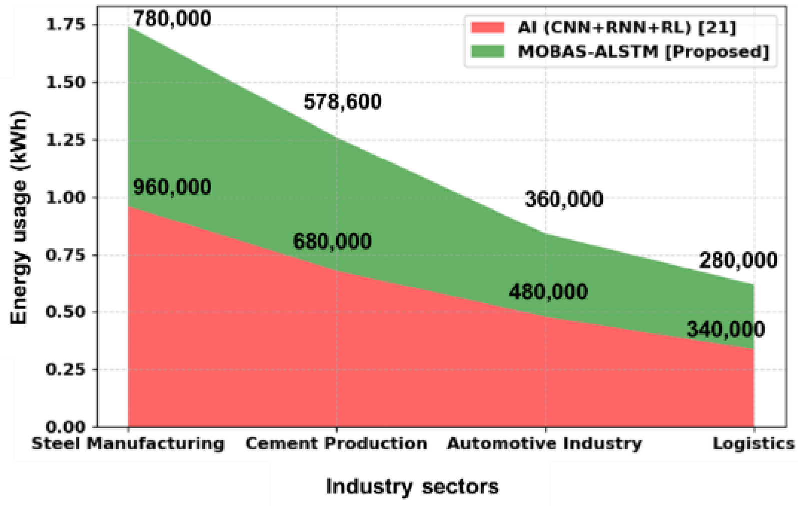

Figure 9: The industry sectors' energy usage reduction values for the proposed method.

Table 6 and Figure 9 show the Energy usage reduction findings across industry sectors employing AI (CNN+RNN+RL), and MOBAS-ALSTM shows the lower energy usage in logistics (280,000), exhibiting superior optimization over existing AI methods.

Table 7: CO2 emission reduction for different companies.

Industry Sectors	AI (CNN+RNN+RL) [21]	MOBAS-ALSTM [Proposed]	Reduction (%)
Steel Manufacturing	256,000	207,000	19.14
Cement Production	176,000	145,600	17.27
Automotive Industry	144,000	130,000	9.72
Logistics	119,000	99,000	16.81

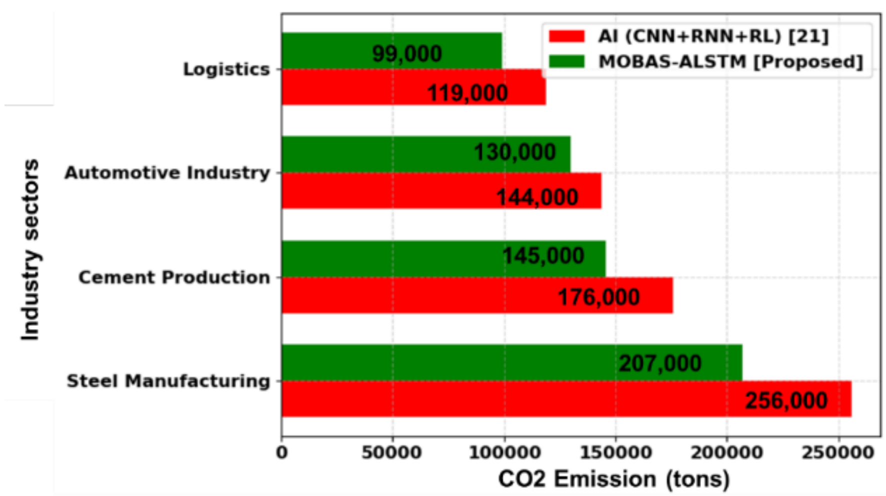

Figure 10: The industry sectors' CO2 emission reduction values for the proposed method.

Table 7 and Figure 10 display the CO2 emission findings employing AI (CNN+RNN+RL) and MOBAS-ALSTM, which demonstrate an outstanding lower CO2 emission in Logistics (99,000) demonstrating the proposed method's effective optimization capacity across several industry sectors.

Table 8: The ART decision-making for different companies.

Industry Sectors	AI (CNN+RNN+RL) [21]	MOBAS-ALSTM [Proposed]
Steel Manufacturing	120	96
Cement Production	110	90
Automotive Industry	105	79
Logistics	98	83

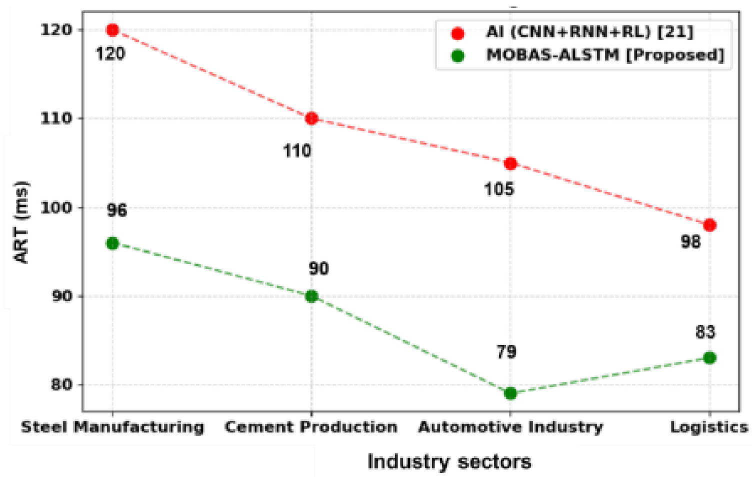

Figure 11: The ART decision-making values for the proposed method in different sectors.

Table 8 and Figure 11 illustrate that ART, MOBAS-ALSTM frequently outperforms AI (CNN+RNN+RL), with the lowest times in the Automotive Industry (79), exhibiting faster decision-making across all sectors.

Table 9: The error metric value compares the proposed vs existing methods.

Metrics	LSTM [22]	ANN [22]	MOBAS-ALSTM [Proposed]
MSE	0.00044	0.0737	0.00030
RMSE	0.020	0.272	0.0173
MAE	0.016	0.190	0.012
R^2	0.997	0.993	0.9985

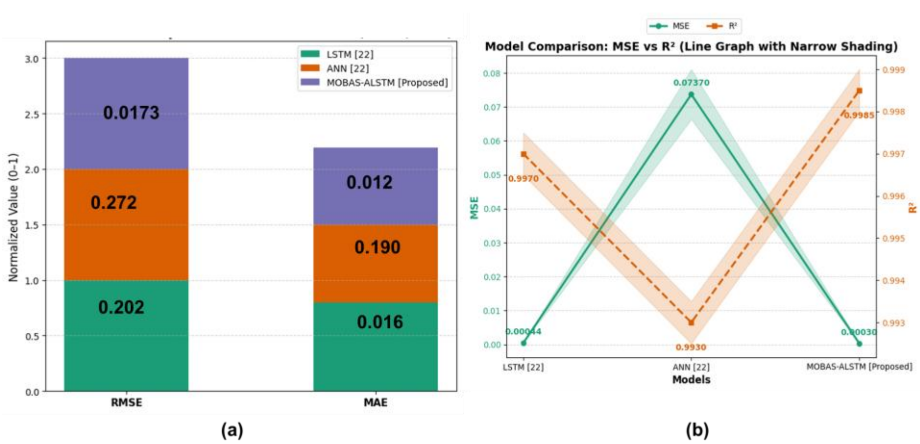

Figure 12 (a-b). The error metric a), RMSE and MAE values and b) MSE and R^2 for the proposed method.

Table 10: Performance comparison using statistical significance (5-fold CV, 80/20 split)

Model	**MSE (mean ± SD)**	**RMSE (mean ± SD)**	**MAE (mean ± SD)**	**R^2 (mean ± SD)**	**p-value vs MOBAS-ALSTM**
ANN [22]	0.021 ± 0.004	0.144 ± 0.008	0.110 ± 0.010	0.87 ± 0.03	< 0.01
LSTM [22]	0.018 ± 0.003	0.134 ± 0.007	0.096 ± 0.009	0.89 ± 0.02	< 0.01
CNN+RNN+RL [21]	0.016 ± 0.002	0.128 ± 0.006	0.090 ± 0.008	0.91 ± 0.02	< 0.05
MOBAS-ALSTM	0.012 ± 0.002	0.110 ± 0.005	0.078 ± 0.007	0.94 ± 0.01	–

Table 9 and Figures 12 (a-b) display that the MOBAS-ALSTM method outperforms LSTM and ANN, with the lowest MSE (0.00030), RMSE (0.0173), MAE (0.012), and highest R^2 (0.9985). The findings show outstanding prediction accuracy, resilience, and reliability, making it ideal for accurate CF forecasting and emission reduction strategy optimization across industries.

Table 10 display the Comparison of results (MSE, RMSE, MAE, R^2) with mean ± SD and p-values from paired t-tests. MOBAS-ALSTM (0.012±0.002 MSE, R^2=0.94) performs significantly better than baselines. Use a paired t-test to compare the MOBAS-ALSTM errors (MSE/MAE, etc.) to each baseline (ANN, LSTM, CNN+RNN+RL). Dataset split: state that you used an 80/20 train-test split and repeated trials with 5-fold cross-validation for robustness. Report the mean ± standard deviation and p-value for the significance test. ALSTM enhances context-sensitive learning, while MOBAS uses Pareto fronts for practical trade-offs. Disclosure of SHAP, temporal-attention diagnostics, and policy perturbations enhances transparency, decision-relevance, and resilience to uncertainty in carbon reduction plans.

The results of the experiment indicated that the proposed method for MOBAS-ALSTM has greater accuracy, stability, and flexibility for forecasting energy use, a decrease in emissions allocation, and accounting for CF compared to AI (CNN + RNN + RL) [21], LSTM [22], ANN [22], and existing methods. MOBAS-ALSTM is a novel method that optimizes performance, supports sustainable operations, and considers environmental regulations, corporate ESG, and operational efficiency, paving the way for intelligent sustainability-centric solutions. MOBAS-ALSTM offers superior sustainability results and forecast accuracy, making it a stable and useful solution for ESG-aligned industrial applications, balancing accuracy with decision-centric optimization.MOBAS-ALSTM unifies diverse IoT/ERP streams, embeds dynamic policy restrictions, and handles missing ESG data through adaptive imputation to enable realistic scalability. Faster convergence and robust Pareto trade-offs are achieved as compared to resilient control approaches, providing dependable, practical decision support for businesses in a variety of regulatory and industrial contexts.

5 Conclusion

The research developed a smart platform for CF accounting and emission reduction strategy optimization for listed companies using MOBAS-ALSTM, combining temporal learning capabilities with MOBAS optimization for accurate forecasting and optimal strategy allocation, overcoming limitations of existing methods like LSTM, ANN, and AI-based CNN+RNN+RL. The experimental results showed that the proposed MOBAS-ALSTM method achieved the lowest MSE (0.00030), RMSE (0.0173), MAE (0.012), and the highest R^2 (0.9985), higher than any of the other methods used for comparison. The proposed framework, despite its limitations, requires more computational power, quality data, and adaptation for real-time analytics deployment in resource-constrained environments. MOBAS-ALSTM uses sector-specific carbon intensity data and adaptive optimization to generalize across industries, incorporating dynamic policy variables like renewable incentives and carbon taxes for practical relevance and regulatory robustness.

ALSTM and MOBAS face challenges like domain shifts, noisy data, and hyperparameter sensitivity. Mitigation strategies include TL uncertainty quantification, surrogate optimization, and online updating. The MOBAS-ALSTM algorithm has limitations in scalability and sensitivity to data drift. It performs well on small datasets but may require parallelization or distributed learning for larger industrial datasets. Future enhancements will include adaptive retraining and drift-detection approaches. Future research should focus on reducing computational complexity, integrating edge computing for real-time industrial deployment, and broadening the model to include multimodal data for improved forecast robustness and scalability.

Availability of data and materials

This study complies data availability policy. Data access arrangements align with the journal's guidelines and can be facilitated through the corresponding author.

Author contributions

Jinhong Song writing original draft preparation & methodology,MengLiu investigation & writing review and editing.

Ethics approval statement

This study utilized publicly available data/literature analysis and did not involve primary data collection from human/animal subjects, exempting it from ethical review.

References

[1] Huang, L., Long, Y., Chen, J., & Yoshida, Y. (2023). Sustainable lifestyle: Urban household carbon footprint accounting and policy implications for lifestyle-based decarbonization. *Energy Policy*, *181*, 113696. https://doi.org/10.1016/j.enpol.2023.113696

[2] Augoye, O., Muyiwa-Ajayi, T. P., & Sobowale, A. (2024). The effectiveness of carbon accounting in reducing corporate carbon footprints. *International Journal of Multidisciplinary Research and Growth Evaluation*, *5*(1), 1364-1371. https://doi.org/10.54660/.IJMRGE.2024.5.1.1364-1371

[3] Ahmetoğlu, S., & Tanık, A. (2020). Management of carbon footprint and determination of GHG emission sources in construction sector. *International Journal of Environment and Geoinformatics*, *7*(2), 191-204. https://doi.org/10.30897/ijegeo.726913

[4] Yu, F., Yuan, Q., Sheng, X., Liu, M., Chen, L., Yuan, X., & Ma, Q. (2024). Understanding carbon footprint: An evaluation criterion for achieving sustainable development. *Chinese Journal of Population, Resources and Environment*, *22*(4), 367-375. https://doi.org/10.1016/j.cjpre.2024.11.001

[5] Wang, L., & Dai, S. (2024). Carbon Footprint Accounting and Verification of Seven Major Urban Agglomerations in China Based on Dynamic Emission Factor Model. *Sustainability*, *16*(22), 9817. https://doi.org/10.3390/su16229817

[6] Ma, Y., Liu, X., Liu, J., Du, C., Liang, M., Li, W., & Wei, B. (2024). Carbon Emission Accounting and Reduction Evaluation in Sponge City Residential Areas. *Water*, *16*(17), 2535. https://doi.org/10.3390/w16172535

[7] Duan, C., Wang, Z., Zhou, B., & Yao, X. (2024). Global polyethylene terephthalate (PET) plastic supply chain resource metabolism efficiency and carbon emissions co-reduction strategies. *Sustainability*, *16*(10), 3926. https://doi.org/10.3390/su16103926

[8] López, B., Rangel-Pérez, C., & Fernández, M. (2023). Sustainable strategies in the luxury business to increase efficiency in reducing carbon footprint. *Journal of Business Research, 157,* 113607. https://doi.org/10.1016/j.jbusres.2022.113607

[9] Zhai, Y., Li, Y., Tang, S., Liu, Y., & Liu, Y. (2024). Lightweight strategies for wooden-structure buildings based on embodied carbon emission calculations for carbon reduction. *Buildings, 14*(11), 3460. https://doi.org/10.3390/buildings14113460

[10] Li, Z., Li, X., Lu, C., Ma, K., & Bao, W. (2024). Carbon emission responsibility accounting in renewable energy-integrated DC traction power systems. *Applied Energy, 355,* 122191. https://doi.org/10.1016/j.apenergy.2023.122191

[11] Hertwich, E. G. (2021). Increased carbon footprint of materials production driven by rise in investments. *Nature Geoscience, 14*(3), 151–155. https://doi.org/10.1038/s41561-021-00690-8

[12] Chen, X., Ma, C., Zhou, H., Liu, Y., Huang, X., Wang, M., Cai, Y., Su, D., Muneer, M. A., Guo, M., & Chen, X. (2021). Identifying the main crops and key factors determining the carbon footprint of crop production in China, 2001–2018. *Resources, Conservation and Recycling, 172,* 105661. https://doi.org/10.1016/j.resconrec.2021.105661

[13] Walenta, J. (2021). The making of the corporate carbon footprint: The politics behind emission scoping. *Journal of Cultural Economy, 14*(5), 533–548. https://doi.org/10.1080/17530350.2021.1935297

[14] Banerjee, S., Khan, M. A., & Ul Husnain, M. I. (2021). Searching appropriate system boundary for accounting India's emission inventory for the responsibility to reduce carbon emissions. *Journal of Environmental Management, 295,* 112907. https://doi.org/10.1007/s42729-021-00587-w

[15] Liu, Z., Sun, T., Yu, Y., Ke, P., Deng, Z., Lu, C., Huo, D., & Ding, X. (2022). Near-real-time carbon emission accounting technology toward carbon neutrality. *Engineering, 14,* 44–51. https://doi.org/10.1016/j.eng.2021.12.019

[16] Yuan, X., Sheng, X., Chen, L., Tang, Y., Li, Y., Jia, Y., Qu, D., Wang, Q., Ma, Q., & Zuo, J. (2022). Carbon footprint and embodied carbon transfer at the provincial level of the Yellow River Basin. *Science of the Total Environment, 803,* 149993. https://doi.org/10.1016/j.scitotenv.2021.149993

[17] Huang, W., Wu, F., Han, W., Li, Q., Han, Y., Wang, G., Feng, L., Li, X., Yang, B., Lei, Y., & Fan, Z. (2022). Carbon footprint of cotton production in China: Composition, spatiotemporal changes and driving

factors. *Science of the Total Environment, 821,* 153407. https://doi.org/10.1016/j.scitotenv.2022.153407

[18] Farago, M., Damgaard, A., Rebsdorf, M., Nielsen, P. H., & Rygaard, M. (2022). Challenges in carbon footprint evaluations of state-of-the-art municipal wastewater resource recovery facilities. *Journal of Environmental Management, 320,* 115715. https://doi.org/10.1016/j.jenvman.2022.115715

[19] Valls-Val, K., & Bovea, M. D. (2022). Carbon footprint assessment tool for universities: CO2UNV. *Sustainable Production and Consumption, 29,* 791–804. https://doi.org/10.1016/j.spc.2021.11.020

[20] García-Alaminos, Á., Gilles, E., Monsalve, F., & Zafrilla, J. (2022). Measuring a university's environmental performance: A standardized proposal for carbon footprint assessment. *Journal of Cleaner Production, 357,* 131783. https://doi.org/10.1016/j.jclepro.2022.131783

[21] Alghieth, M. (2025). Sustain AI: A multi-modal deep learning framework for carbon footprint reduction in industrial manufacturing. *Sustainability, 17*(9), 4134. https://doi.org/10.3390/su17094134

[22] Ezenkwu, C. P., Cannon, S., & Ibeke, E. (2024). Monitoring carbon emissions using deep learning and statistical process control: A strategy for impact assessment of governments' carbon reduction policies. *Environmental Monitoring and Assessment, 196*(3), 231. https://doi.org/10.1007/s10661-024-12388-6

[23] Boulkroune, A., Zouari, F., & Boubellouta, A. (2025). Adaptive fuzzy control for practical fixed-time synchronization of fractional-order chaotic systems. *Journal of Vibration and Control.* Advance online publication. https://doi.org/10.1177/10775463251320258

[24] Boulkroune, A., Hamel, S., Zouari, F., Boukabou, A., & Ibeas, A. (2017). Output-feedback controller based projective lag-synchronization of uncertain chaotic systems in the presence of input nonlinearities. *Mathematical Problems in Engineering, 2017,* 8045803. https://doi.org/10.1155/2017/8045803

[25] Zouari, F., Saad, K. B., & Benrejeb, M. (2012). Robust neural adaptive control for a class of uncertain nonlinear complex dynamical multivariable systems. *International Review on Modelling and Simulations, 5*(5), 2075–2103. https://doi.org/10.1016/j.isatra.2021.11.007

[26] Zouari, F., Saad, K. B., & Benrejeb, M. (2013, March). Adaptive backstepping control for a class of uncertain single input single output nonlinear systems. In *2013 10th International Multi-Conferences on Systems, Signals & Devices (SSD13)* (pp. 1–6). IEEE. https://doi.org/10.1109/SSD.2013.6564134

[27] Rigatos, G., Abbaszadeh, M., Sari, B., Siano, P., Cuccurullo, G., & Zouari, F. (2023). Nonlinear optimal control for a gas compressor driven by an induction motor. *Results in Control and Optimization, 11,* 100226. https://doi.org/10.1016/j.rico.2023.100226

[28] Li, Y., Tong, S., & Li, T. (2013). Adaptive backstepping control for a single-link flexible robot manipulator driven DC motor. In *2013 International Conference on Control, Decision and Information Technologies (CoDIT)* (pp. 668–673). IEEE. https://doi.org/10.1109/CoDIT.2013.6689656

[29] Wang, Z., & Guo, J. (2025). Adaptive convolutional residual network for dual-task forecasting in energy market planning. *Informatica, 49*(24). https://doi.org/10.31449/inf.v49i24.8032